Articles

Time-Resolved Rotational Dynamics of Phosphorescent-Labeled Myosin Heads in Contracting Muscle Fibers[†]

Richard A. Stein, Richard D. Ludescher,[‡] Peter S. Dahlberg, Piotr G. Fajer, Robert L. H. Bennett, and David D. Thomas*

Department of Biochemistry, University of Minnesota Medical School, Minneapolis, Minnesota 55455
Received March 22, 1990; Revised Manuscript Received July 17, 1990

ABSTRACT: We have measured the microsecond rotational motions of myosin heads in contracting rabbit psoas muscle fibers by detecting the transient phosphorescence anisotropy of eosin-5-maleimide attached specifically to the myosin head. Experiments were performed on small bundles (10–20 fibers) of glycerinated rabbit psoas muscle fibers at 4 °C. The isometric tension and physiological ATPase activity of activated fibers were unaffected by labeling 60–80% of the heads. Following excitation of the probes by a 10-ns laser pulse polarized parallel to the fiber axis, the time-resolved emission anisotropy of muscle fibers in rigor (no ATP) showed no decay from 1 μs to 1 ms (r_∞ = 0.095), indicating that all heads are rigidly attached to actin on this time scale. In relaxation (5 mM MgATP but no Ca^{2+}), the anisotropy decayed substantially over the microsecond time range, from an initial anisotropy (r_0) of 0.066 to a final anisotropy (r_∞) of 0.034, indicating large-amplitude rotational motions with correlation times of about 10 and 150 μs and an overall angular range of 40–50°. In isometric contraction (MgATP plus saturating Ca^{2+}), the amplitude of the anisotropy decay (and thus the amplitude of the microsecond motion) is slightly less than in relaxation, and the rotational correlation times are about twice as long, indicating slower motions than those observed in relaxation. While the residual anisotropy (at 1 ms) in contraction is much closer to that in relaxation than in rigor, the initial anisotropy (at 1 μs) is approximately equidistant between those of rigor and relaxation. Therefore, the anisotropy decay in contraction is not a simple linear combination of those in rigor and relaxation, implying that there are myosin head rotations in contraction that are distinct from those in both rigor and relaxation. Fiber stiffness in isometric contraction is about 70% of the rigor value, suggesting that a majority of cross-bridges are attached to actin. Therefore, much of the rotational motion observed in contraction probably occurs in the attached phase of the cross-bridge cycle.

Muscle contraction requires movement of the myosin cross-bridge, which consists of two globular actin-binding myosin "heads" (S1) connected to the thick filament by a single rodlike domain (S2). Motions involving molecular rotation of or within S1, elastic deformation of S2, or helix-coil transitions within S2 have all been postulated [review by Cooke (1986)]. Much structural, biochemical, and mechanical evidence supports such motions, but most of this evidence is indirect, serving only to establish the plausibility of flexible cross-bridge mechanisms. Some of the most direct information about cross-bridge orientation and rotational motion, and their role in force generation, has come from spectroscopic molecular probes. These probes have three properties that no other method combines [review by Thomas (1987)]: (1) They can be attached covalently and specifically to myosin heads, so that the information comes directly and exclusively from heads.

(2) Through a judicious choice of the probe and the instrument, signals can be detected that provide information only about *rotation*, the type of motion postulated in most muscle theories. (3) The measurements of these motions can be made under physiological conditions during muscle action.

Spectroscopic studies of myosin head rotation usually involve a paramagnetic or optical probe covalently attached to the fast reacting sulfhydryl (SH1) in the myosin head (Thomas, 1987). These studies have established several important conclusions about cross-bridge motion. Cross-bridges in synthetic filaments are flexible, allowing heads to undergo thermally driven fluctuations of large amplitude. Fluorescence anisotropy studies, limited to the nanosecond time range, established that myosin heads can wobble independently of the coiled-coil tail in myosin monomers (Mendelson et al., 1973, 1975). Saturation-transfer EPR,[1] with sensitivity to both nanosecond and microsecond motions, confirmed the fluorescence results and showed that microsecond cross-bridge flexibility occurs in myosin filaments (Thomas et al., 1975, 1980). Absorption and phosphorescence studies, using long-lived triplet probes,

[1] Abbreviations: CP, creatine phosphate; CPK, creatine phosphokinase; DTT, dithiothreitol; E5M, eosin-5-maleimide; EGTA, ethylene glycol bis(β-aminoethyl ether)-*N,N,N',N'*-tetraacetic acid; EDTA, ethylenediaminetetraacetic acid; EPR, electron paramagnetic resonance; MOPS, 3-(*N*-morpholino)propanesulfonic acid; TAA, transient absorption anisotropy; TPA, transient phosphorescence anisotropy.

combined microsecond sensitivity with time resolution to provide more detailed information about these motions of heads in filaments, showing that the head wobble is restricted in amplitude and that at least two modes of microsecond motion occur (Eads et al., 1984; Kinosita et al., 1984; Ishiwata et al., 1987; Ludescher et al., 1988). These studies clearly demonstrated that cross-bridge flexibility is inherent in the myosin structure. The motion is complex, probably representing segmental rotations of the head (S1) and part of the rod (S2).

Myosin heads in relaxed myofibrils are rotationally mobile. Although fluorescence studies of myofibrils detected little mobility in the nanosecond time scale (Mendelson & Cheung, 1976), saturation-transfer EPR revealed microsecond head rotations in relaxed myofibrils, comparable to the motions in filaments made from purified myosin (Thomas et al., 1980). Studies with phosphorescent probes confirmed this microsecond mobility, resolved at least two correlation times, and showed that the motion is restricted only slightly compared to that seen in solution (Ishiwata et al., 1987; Ludescher & Thomas, 1988).

Myosin heads bind rigidly to actin in the absence of nucleotides. In solution, actin eliminates virtually all nanosecond rotations of myosin heads, as detected by fluorescence (Mendelson et al., 1973; Highsmith et al., 1976), and the microsecond motions are greatly restricted, as detected by ST-EPR (Thomas et al., 1979, 1980) and absorption anisotropy measurements with phosphorescent probes (Eads et al., 1984; Kinosita et al., 1984). Even more profound immobilization has been consistently observed in myofibrils, apparently due to more rigid actin filaments, as detected by ST-EPR (Thomas et al., 1980) and phosphorescence (Ishiwata et al., 1987; Ludescher & Thomas, 1988).

Direct insight into the role of cross-bridge flexibility in the force generating event, however, requires measurements on intact muscle fibers. Spectroscopic studies of muscle fibers have so far employed only paramagnetic or fluorescent probes. The orientational resolution of conventional EPR has been used to show that myosin heads are highly oriented in rigor and highly disoriented in relaxation (Thomas & Cooke, 1980) and that in contraction most heads are in a disoriented population but a small fraction has a rigorlike orientation (Cooke et al., 1982). Saturation-transfer EPR, which is sensitive to microsecond motions, indicates that the disorder seen in relaxation (Fajer et al., 1988) and contraction (Barnett & Thomas, 1989; Fajer et al., 1990) is dynamic on the microsecond time scale. However, these measurements lack the time resolution needed to characterize fully the complex rotations expected to occur during the active cross-bridge cycle. Time-resolved fluorescence anisotropy studies of cross-bridge motion in fibers are limited to the nanosecond time range, due to the short excited-state lifetimes of singlet probes (Burghardt & Thompson, 1985; Burghardt & Ajtai, 1985). Therefore, we report here phosphorescence emission anisotropy measurements of the microsecond rotational motions of eosin-labeled myosin heads in glycerinated rabbit psoas muscle fibers in the physiological states of rigor, relaxation, and contraction. These are the first time-resolved measurements of cross-bridge motion in fibers in the physiologically important time range from 1 to 1000 μs.

Materials and Methods

Reagents and Solutions. Eosin-5-maleimide (E5M) was obtained from Molecular Probes (Eugene, OR) and stored at a concentration of 2 mM in dimethylformamide (DMF) at −70 °C. Glycerol was from Fisher Scientific (Pittsburgh, PA). Catalase, glucose oxidase, glucose, ATP, creatine phosphate (CP), and creatine phosphokinase (CPK) were from Sigma

(St. Louis, MO). All chemicals were of the highest available purity. The following solutions were used in our experiments: washing solution (W) 20 mM MOPS, 120 mM KAc, 1 mM EGTA, 2 mM MgCl$_2$, 0.1 mM NaN$_3$; labeling solution (L) W + 5 mM PP$_i$ + 5 mM MgCl$_2$; rigor solution (R) 84 mM KPr, 25 mM MOPS, 2 mM MgCl$_2$, 1 mM EGTA, 10 mM CP; rigor solution plus backup (RI) R + 583 units of CPK/mL; relaxation solution plus backup (RE) RI + 5 mM ATP; contraction solution (C) RE + 1.5 mM CaCl$_2$. The ionic strength of RE was 154 mM.

Preparations. Glycerinated rabbit psoas fibers were prepared and stored at −20 °C for up to 3 months (Ludescher & Thomas, 1988; Fajer et al., 1988). Myofibrils were made by homogenizing fibers (Ludescher & Thomas, 1988). Fibers were labeled with E5M by a procedure similar to that described previously (Ludescher & Thomas, 1988). Bundles of glycerinated fibers about 0.2–0.4 mm thick were tied to glass rods and washed with solution W to remove glycerol. Membrane debris was removed by soaking fibers for 15 min in solution W plus 0.5% Triton X-100 and 0.1 mM DTT. The fibers were then washed three times (10 min each) with solution W. After a 15-min prelabeling wash in solution L, E5M was added at a final concentration of 4 μM, and the fibers were labeled for 60 min. The reaction was quenched for 15 min with solution L plus 4 mM DTT. The fibers were washed three times (10 min each) in solution W and then stored in solution W plus 50% glycerol and 0.1 mM DTT at −20 °C for up to 3 months without significant changes in spectroscopic, mechanical, or biochemical properties.

Biochemical and Mechanical Assays. Protein concentration was measured with a Biuret assay modified from that of Gornall et al. (1949). Protein at a concentration of 1–6 mg/mL was incubated in a solution containing 1.5% CuSO$_4$, 6% sodium potassium tartarate, 30% NaOH (w/v), and 2% Sterox (v/v) for 15 min, and the absorbance was measured at 310 nm. Bovine serum albumin, assayed by the same procedure, was used as a standard. To determine the amount of eosin incorporated, myofibrils made from eosin-labeled fibers were dissolved in 0.5 M KCl. Urea was then added to a final concentration of 5 M, and the solution was then spun at 1000g for 10 min at 0 °C. The protein concentration of the supernatant was measured by the Biuret assay, and the amount of eosin incorporated was calculated by measuring the absorbance at 530 nm (E_{530} = 97 000 M^{-1} cm^{-1}). The extinction coefficient was calculated by allowing a known concentration of dye to react to completion with myofibrils, which where then treated as above, and then measuring the absorbance at 530 nm. The mole ratio of eosin bound per head (dye/head) was calculated as described previously (Ludescher & Thomas, 1988), assuming that 50% of the protein is myosin. The ATPase activity of myofibrils made from fibers was measured by monitoring the inorganic phosphate release, as previously described (Eads et al., 1984). The fraction (f_{SH}) of the labeled fast-reacting thiols in the 20-kDa domain of myosin (SH1, Cys 707, or SH2, Cys 697) was determined as the fractional inhibition of the K/EDTA ATPase (Ludescher et al., 1988). The specificity of labeling, i.e., the fraction of bound labels that are bound to these SH groups, was determined as f_{SH}/(dye/head). This is a lower bound for the fraction of bound labels that are bound to the 20-kDa domain of the myosin head.

Force measurements were made on single fibers by using an Akers force transducer (Fajer et al., 1988). The tension was calculated by dividing the measured force by the cross-sectional area of the fiber, as measured with a stereo micro-

scope. Stiffness was measured as described previously (Fajer et al., 1988), except that the force transducer was Model FXA-0 from Cambridge Technology (Cambridge, MA).

Spectroscopic Experiments. Small fiber bundles (approximately 0.2 mm in diameter) in solution W/50% glycerol were glued to a support that fits diagonally in a 1-cm cuvette (Burghardt & Thompson, 1985) and bathed in R solution. The fibers were oriented vertically, parallel to the excitation polarization, and the bathing solution was deoxygenated prior to data collection by an enzymatic procedure (Eads et al., 1984). The cuvette was covered with parafilm, and the air above the solution was displaced continuously with a nitrogen purge. Deoxygenation of the fibers occurred within 15 min, as indicated by a high and stable phosphorescence yield. To obtain relaxation, the fibers were first deoxygenated in 2 mL of RI solution, and then 106 μL of 100 mM MgATP was added through the paraffin with a Hamilton syringe and mixed with the solution; the fibers were allowed to equilibrate with the new solution for 5 min before data acquisition. This was sufficient to obtain saturation with ATP and deoxygenation. Isometric contraction was induced by addition of 30 μL of 100 mM CaCl$_2$, and this was also allowed to equilibrate for several minutes before data acquisition.

Time-resolved phosphorescence emission was measured as described by Ludescher and Thomas (1988), except that the photomultiplier gating was transmitted from the laser power supply via a fiber optic cable, to minimize radio frequency interference. The phosphorescence emission decays polarized parallel ($I_\parallel$) and perpendicular ($I_\perp$) to the vertical excitation polarization were collected through a Polaroid sheet polarizer. Data acquisition and signal averaging were controlled by a LeCroy 3500 multichannel analyzer using a CAMAC interface. Each decay (1024 channels) was digitized by photon counting, using a LeCroy multichannel scalar (Model 3521) that has a time resolution of 1 μs or greater per channel. A typical anisotropy experiment consisted of collecting decays from 2000 laser pulses, with the emission polarizer first vertical and then horizontal (a single loop), and repeating this for 15–25 loops. Since the laser was typically operated at a repetition rate of 100 Hz, each experiment lasted about 10–15 min. Repeat experiments with the same sample were virtually identical, and the functional properties of labeled fibers were preserved, ruling out photochemical artifacts.

The excited-state lifetimes were determined from the total (unpolarized) intensity decay, $I(t) = I_\parallel + 2GI_\perp$, where G is a correction factor determined in control experiments on an isotropic sample (1 μM E5M in solution). Alternatively, $I(t)$ was obtained by placing the emission polarizer at the magic angle (54.7°) with respect to vertical, with identical results. The rotational correlation times were determined from the anisotropy decay, $r(t) = (I_\parallel - GI_\perp)/I(t)$.

Analysis of Phosphorescence Data. $I(t)$ was analyzed by a nonlinear least-squares fit to a sum of exponentials plus a constant background (Ludescher et al., 1988). When this background is subtracted, the function becomes

$$I(t) = \sum_{i=1}^{n} a_i \exp(-t/\tau_i) \tag{1}$$

where τ_i is the excited-state lifetime for component i. The anisotropy decay was fit to a sum of exponential plus a constant (Ludescher & Thomas, 1988)

$$r(t) = \sum_{i=1}^{n} r_i \exp(-t/\phi_i) + r_\infty \tag{2}$$

where $r_0 = r(0)$ is the initial anisotropy and ϕ_i is the rotational

correlation time for component i. The number of exponentials (n in eq 1 or 2) was increased until no further improvement was observed in the fit, as evaluated from the modified χ^2 value (minimized in the least-squares fit) and the residual plot (data minus fit). For $I(t)$, we found consistently that the fit was improved by increasing n from 2 to 3, but not by increasing n to 4. For $r(t)$, $n = 2$ was usually both necessary and sufficient for an optimal fit.

Time-resolved phosphorescence anisotropy allows for the analysis of the rates (diffusion coefficients, which are inversely proportional to the observed correlation times ϕ_i in eq 2) and angular amplitudes (roughly proportional to the amplitudes r_i in eq 2) of probe rotational motions. The proportionality constants depend on the type of anisotropic motion that is occurring (Zannoni et al., 1983; Burghardt, 1985). The amplitudes of the anisotropy decay depend on the amplitudes of the rotation and the orientation of the probe relative to the fiber axis (Zannoni et al., 1983; Vogel & Jähnig, 1985). In a randomly oriented system, r_0 is determined by the angle between the excitation and emission dipoles and by the amplitudes of motions too fast to detect (in this case, $\phi \leq 1$ μs), while the amplitude of decay to r_∞ depends on the *dynamic disorder*, determined by the amplitudes of rotations in the detected time window (in this case, 1 μs $\leq \phi \leq 1$ ms). In an oriented system, such as oriented fibers, r_0 and r_∞ are affected by the same factors, but also by the *static orientation*, determined by the amplitudes of probe rotations slower than the detected time window (in this case, $\phi > 1$ ms).

In the case of vertically oriented fibers, only axial rotations, which change the angle between the vertical (fiber) axis and the emission transition moment, are detectable. Azimuthal rotations, rotations about the fiber axis, are not detectable. We analyzed r_0 and r_∞ using the formalism developed by Vogel and Jähnig (1985). In this analysis, r_0 and r_∞ are expressed in terms of two types of order parameters, which define the static orientation and dynamic disorder. For the experiments in the present study, in which the exciting light is polarized vertically (parallel to the fibers), the relevant expressions are

$$r_0 = \frac{(55/35)\langle P_2\rangle_s\langle P_2\rangle_d - (36/35)\langle P_4\rangle_s\langle P_4\rangle_d + (2/5)}{1 + 2\langle P_2\rangle_s\langle P_2\rangle_d} r_0(\text{MF}) \tag{3}$$

$$r_\infty = [(\langle P_2\rangle_s\langle P_2\rangle_d + (36/35)\langle P_4\rangle_s\langle P_2\rangle_d{}^2 + (20/35) \times \langle P_2\rangle_s\langle P_2\rangle_d{}^2 + (2/5)\langle P_2\rangle_d{}^2)/(1 + 2\langle P_2\rangle_s\langle P_2\rangle_d)]r_0(\text{MF}) \tag{4}$$

where the subscript d denotes dynamic disorder, due to rotational motions occurring in the observed time window (between 1 μs and 1 ms), and the subscript s indicates static orientation, due to rotations slower than 1 ms. The static orientation is defined relative to the fiber axis, whereas the dynamic disorder is relative to the director of the static orientation. The order parameters are ensemble averages (indicated by angled brackets), over the appropriate time windows, of the Legendre polynomials $P_2 \equiv P_2(\cos\Theta_i) \equiv (3\cos^2\Theta_i - 1)/2$ and $P_4 \equiv P_4(\cos\Theta_i) \equiv (35\cos^4\Theta_i - 30\cos^2\Theta_i + 3)/8$, where Θ_i is either Θ_d or Θ_s. Equations 3 and 4 are derived directly from the expressions of Vogel and Jähnig (1985), with the addition of $r_0(\text{MF})$, the r_0 value obtained from the anisotropy decay of myofibrils in rigor, which accounts for any submicrosecond disorder and the angle between the absorption and emission moments.

Since there are four unknown order parameters ($\langle P_2\rangle_s$, $\langle P_4\rangle_s$, $\langle P_2\rangle_d$, $\langle P_4\rangle_d$) but only two observables (r_0 and r_∞), we must assume a model for the disorder to estimate the angular
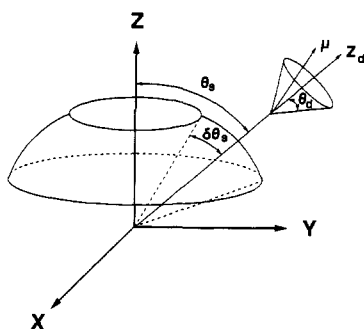
FIGURE 1: Definition of the angular amplitudes used to analyze the anisotropy decays, including both the dynamic disorder and static orientation. The emission transition moment, μ, is assumed to wobble within a cone of semiangle Θ_d within the observed time window of 1 μs–1 ms. The director of this cone, Z_d, is confined within a band centered at Θ_s relative to the fiber axis, with a half-width of $\delta\Theta_s$, defining the static disorder that is assumed to occur on a time scale longer than 1 ms.

Table I: Labeling Extent and Specificity[a]

| sample | ATPase activity (IU) | | dye/head | specificity |
	K/EDTA	Ca/EDTA		
unlabeled	0.637	0.075		
	(0.021)	(0.004)		
labeled	0.205	0.146	0.69	0.98
	(0.024)	(0.007)	(0.03)	(0.02)

[a] All ATPase activities were measured at 25 °C in the media described under Materials and Methods, using myofibrils made by homogenizing labeled or unlabeled fiber bundles. The units (IU) for ATPase activities are μmol of P_i released min^{-1} (mg of protein)$^{-1}$. The specificity is defined as the fraction of SH groups labeled (the fractional inhibition of the K/EDTA ATPase) divided by the dye/head ratio (determined from optical absorption). Unlabeled fibers went through the labeling procedure except for the E5M. The numbers in parentheses indicate the ranges of duplicate measurements.

amplitudes. We assume that the dynamic disorder of the emission transition moment is described by a wobble in a cone (with semiangle Θ_d), where the center of the cone (defined by the axis Z_d) must lie within the angular range defined by the static orientation, centered at Θ_s, with a width of $\delta\Theta_s$ (Figure 1). Integration of the Legendre polynomials over these angular ranges yields values of the four order parameters, and eqs 3 and 4 can then be used to obtain expressions for r_0 and r_∞ in terms of the three angles (Θ_s, $\delta\Theta_s$, and Θ_d). A search was performed over all possible values of these angles (with a 1° resolution), to determine which values are consistent with the observed values of r_0 and r_∞. We found that we could determine the dynamic disorder Θ_d uniquely, but not the static orientation (defined by Θ_s and $\delta\Theta_s$). The result is a probability distribution for Θ_d, with the peak of the distribution determining Θ_d and the width of the distribution equal to the uncertainty in this angle. To define unambiguously Θ_s and $\delta\Theta_s$, experiments would have to be performed at several different orientations of the fiber axis with respect to the excitation polarization (Vogel & Jähnig, 1985).

RESULTS

Extent and Specificity of Labeling. For a typical E5M-labeled fiber preparation, 0.69 ± 0.03 molecules of eosin were covalently bound per myosin head, as measured from the dye absorbance (Table I). The K/EDTA ATPase activity was inhibited by 68% ± 0.02, so 98 ± 6% (0.68/0.69) of the eosin in labeled fibers is attached to SH1 or SH2, in the 20-kDa domain of the myosin head (Table I).

Functional Properties of Labeled Fibers. The physiological characteristics of labeled and control fibers at 4 °C are similar

Table II: Physiological Characterization of Eosin-Labeled Fibers[a]

| sample | relaxation | | contraction | |
	ATPase (IU)	tension (kg/cm²)	ATPase (IU)	tension (kg/cm²)
unlabeled	0.003	0.013	0.018	1.24
	(0.001)	(0.006)	(0.001)	(0.11)
labeled	0	0.14	0.016	1.33
	(0.001)	(0.09)	(0.002)	(0.08)

[a] All measurements were made at 4 °C, in the same media used in spectroscopy. The units (IU) for ATPase activities are μmol of P_i released min^{-1} (mg of protein)$^{-1}$. Unlabeled fibers went through the labeling procedure except for the E5M. The numbers in parentheses are the standard errors of the mean, with $n = 5$.
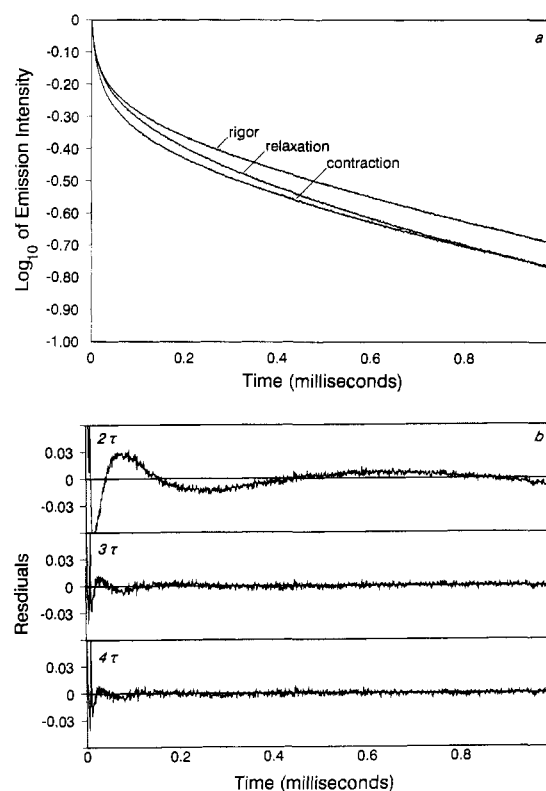

FIGURE 2: Transient phosphorescence intensities $I(t)$ at 4 °C of E5M-labeled fibers in rigor, relaxation, and contraction. $I(t)$ was determined from the same raw data sets [$I_\parallel(t)$ and $I_\perp(t)$] used to calculate the anisotropy decays (Figure 3). Each curve is the average of nine data sets, superimposed on the fit to a three-exponential function (eq 1 with $n = 3$). The results of the fits are shown in Table III. The residuals for two-, three-, and four-exponential fits are plotted for contraction, showing that the three-exponential fit is optimal. The residual plots for rigor and relaxation are similar to those of contraction (data not shown).

(Table II) and are in agreement with previously reported values at 6 °C for unlabeled fibers (Yanagida et al., 1982). The tension in the absence of Ca is slightly higher for labeled than for unlabeled fibers (Table II), probably due to a change in the interaction between myosin and actin caused by SH modification (Svensson & Thomas, 1986; Titus et al., 1989). In the presence of calcium, both the tension and ATPase are unaffected by labeling with E5M, suggesting that the interactions of the active cross-bridge with actin are essentially normal. In particular, it is likely that the labeled cross-bridge is undergoing the same motions as the unlabeled cross-bridge.

Phosphorescence Intensity Decay. The phosphorescence emission intensity decays obtained with unpolarized excitation and detection, $I(t)$, of E5M-labeled muscle fibers at 4 °C in rigor, relaxation, and contraction are shown in Figure 2. These curves do not decay to zero in 1 ms, due to the presence

Table III: Phosphorescence Emission Decay Parameters for Eosin-Labeled Muscle Fibers[a]

state	a_1	τ_1	a_2	τ_2	a_3	τ_3	χ^2
rigor	0.272	10.1	0.221	73.6	0.507	745	1.93
	(0.009)	(0.1)	(0.003)	(1.4)	(0.008)	(33)	(0.04)
relaxation	0.282	10.2	0.239	72.9	0.474	582	2.04
	(0.007)	(0.2)	(0.007)	(2.0)	(0.012)	(13)	(0.03)
contraction	0.346	10.7	0.236	69.2	0.416	629	2.10
	(0.006)	(0.1)	(0.007)	(1.7)	(0.011)	(18)	(0.06)

[a] Nonlinear least-squares fit of the (unpolarized) phosphorescence intensity decay $I(t)$ to a sum of exponential decay terms with amplitudes a_i and excited-state lifetimes τ_i (eq 1). The values are averages from nine experiments, and the numbers in parentheses are the standard errors of the mean. The average decays of these data sets are shown in Figure 1. This table shows only the results for three-exponential fits ($n = 3$ in eq 1), which were judged to be optimal on the basis of residual plots (Figure 2) and χ^2 values.

of a long-lifetime component; measurements over 10 ms do decay to zero (data not shown). Although the three-exponential fits to the data in Figure 2 (Table III) show that ATP and/or calcium have a slight effect on the long-lifetime component (τ_3), the changes are not enough to account for the large differences in the anisotropy decays reported below (Ludescher, 1984; Ludescher et al., 1987b).

The multiexponential character of $I(t)$ in fibers does not imply site heterogeneity. Extracted myosin shows the same complex distribution of lifetimes as the fibers (Ludescher & Thomas, 1988), and eosin displays complex decay behavior in numerous other protein systems. Such behavior occurs when the reactive group is iodoacetamide (Eads et al., 1984), maleimide (Jovin et al., 1981; Ludescher & Thomas, 1988), or isothiocyanate (Austin et al., 1979) and when the labeled protein is water soluble (Cherry et al., 1976) or membrane bound (Bürkli & Cherry, 1981). The case of a single-exponential decay for eosin bound to a protein is quite rare (Garland & Moore, 1979).

Phosphorescence Anisotropy Decay. The anisotropy decays for fibers in rigor, relaxation, and contraction are shown in Figure 3. The anisotropy in rigor is essentially flat with a slight upward rise. This rise is also seen in randomly oriented myofibrils in rigor (Ludescher & Thomas, 1988) and is probably due to lifetime heterogeneity; if a short-lifetime component has a smaller constant value for the anisotropy than a longer lifetime component, then the changing weighted average of the two components will give a rising anisotropy (Ludescher, 1984; Ludescher et al., 1987b). Despite this complication, it is clear that the myosin heads are immobile
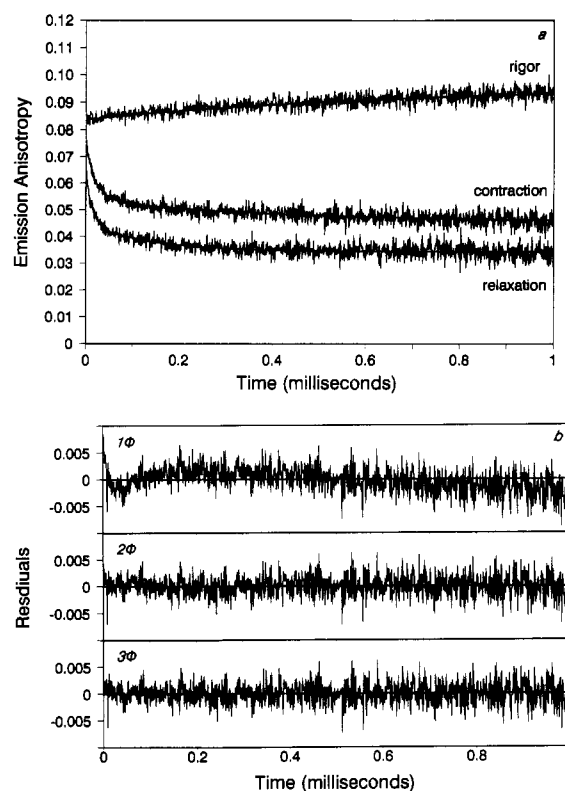

FIGURE 3: Transient phosphorescence anisotropy at 4 °C of E5M-labeled fibers in rigor, relaxation, and contraction, under the same conditions as in Figure 2. Each curve is the average of nine data sets, superimposed on the fit to a two-exponential function (eq 2 with $n = 2$). The results of the fits are shown in Table IV. The residuals for one-, two-, and three-exponential fits are plotted for contraction, showing that the two-exponential fit is optimal. The residual plots for rigor and relaxation are similar to those of contraction (data not shown).

on the time scale from 1 to 1000 μs.

Relaxation, induced by the addition of 5 mM MgATP to the rigor solution, induces complex rotational motion of the E5M-labeled heads. The anisotropy decay (Figure 3) can be fit by either a one-, two-, or three-exponential function (eq 2 with $n = 1, 2,$ or 3). Increasing n from 1 to 2 improves the χ^2 value slightly (Table IV) and clearly improves the residual plot in the early channels (Figure 3). However, no further improvement was obtained by increasing n to 3 (Figure 3), so our further discussion focuses on the two-exponential fit. The major decay component, representing about two-thirds of the microsecond decay amplitude, has a correlation time

Table IV: Phosphorescence Anisotropy Parameters for Eosin-Labeled Muscle Fibers[a]

state	r_1	ϕ_1	r_2	ϕ_2	r_∞	r_0	χ^2
rigor	−0.012	260			0.093	0.081	1.092
	(0.006)	(69)			(0.003)	(0.003)	(0.022)
	−0.011	15.0	−0.009	468	0.095	0.075	1.066
	(0.003)	(3.7)	(0.001)	(83)	(0.004)	(0.004)	(0.022)
relaxation	0.022	55.1			0.035	0.057	1.058
	(0.001)	(6.8)			(0.001)	(0.002)	(0.018)
	0.020	12.0	0.012	167	0.034	0.066	1.022
	(0.002)	(2.2)	(0.001)	(35)	(0.001)	(0.002)	(0.015)
contraction	0.021	70.9			0.048	0.069	1.115
	(0.002)	(8.3)			(0.003)	(0.004)	(0.021)
	0.019	19.3	0.010	311	0.046	0.075	1.058
	(0.002)	(1.4)	(0.001)	(39)	(0.003)	(0.004)	(0.016)

[a] Nonlinear least-squares fit of the anisotropy decay $r(t)$ to a sum of exponential decay terms with amplitudes r_i and rotational correlation times ϕ_i (eq 2). The values are averages from nine experiments, and the numbers in parentheses are the standard errors of the mean. The average decays are shown in Figure 3. Results are shown for both one- and two-exponential functions ($n = 1$ and 2 in eq 2). The two-exponential fits were judged to be optimal, on the basis of the lower χ^2 values and flatter residual plots (Figure 3).

of 12 μs. The remainder of the decay has a correlation time of 167 μs. The initial anisotropy (r_0) is substantially lower in relaxation than in rigor, indicating that the submicrosecond ($\phi \leq 1$ μs) disorder is greater and/or the static ($\phi > 1$ ms) orientation is different in relaxation (Vogel & Jähnig, 1985). The nonzero value of the residual anisotropy (r_∞ in eq 2), which is unaffected by the number of fit components (Table IV), indicates that the microsecond rotational motion of the heads is restricted in angular amplitude.

Contraction also induces complex rotational motion of the cross-bridge. As in relaxation, the decay can be fit by either a one-, two-, or three-exponential function, with two exponentials required to obtain an optimal fit (Figure 3 and Table IV). Contraction differs from relaxation in having (a) higher values for both the initial and residual anisotropies, indicating that the orientational order is greater in contraction than in relaxation and (b) longer correlation times, indicating slower rotational motions.

To ensure that saturating concentrations of ATP were available throughout the muscle fiber bundle during data acquisition, we included an ATP-regenerating system, consisting of creatine phosphate (CP) and creatine phosphokinase. We characterized this system by detecting the phosphorescence anisotropy decay in contraction, varying [CPK] and [CP]. Increasing [CPK] above 583 units/mL had no effect, implying that [CPK] was at a saturating level. We then varied [CP], keeping the ionic strength constant by varying [KPr]. Increasing [CP] from 0 to 5 mM caused a significant decrease in r_∞ from 0.065 ± 0.002 to 0.050 ± 0.002; the higher value is probably due to the presence of some rigor cross-bridges at 0 mM CP. However, further increases in [CP] up to 20 mM had no effect on r_∞ or any other anisotropy parameter, indicating that CP (and hence also ATP) is saturating under our standard conditions (10 mM CP).

DISCUSSION

The time-resolved phosphorescence anisotropy of eosin-maleimide, attached to myosin heads in muscle fibers, does not decay in rigor, indicating a rigid, immobile cross-bridge in the time window from 1 μs to 1 ms (Figure 3). In relaxation, the initial anisotropy is substantially lower, and the heads undergo rotational motions characterized by correlation times of 12 and 170 μs. The nonzero residual anisotropy in relaxation indicates that these microsecond motions are restricted in angular amplitude. In contraction, the initial and final anisotropies have intermediate values, and the rotational motions are substantially slower ($\phi = 19$ and 310 μs) than in relaxation. Further analysis is needed to obtain estimates for the angular amplitudes of these motions and to relate these motions to the complex cross-bridge cycle.

Angular Amplitudes. The r_0 and r_∞ values obtained from the two-exponential fits in Table IV can be analyzed to determine the amplitude of axial rotations in the microsecond time window, as characterized by the cone semiangle Θ_d (Figure 1), by using eqs 3 and 4. Assuming a single cone of rotational motion, the values of Θ_d in relaxation and contraction were 22 ± 2° and 21 ± 1°, respectively (Table V). Thus, the overall amplitudes of microsecond rotational motion are very similar in relaxation and contraction. These amplitudes are both large, suggesting large-scale rotational motions of the head, in agreement with previous EPR measurements in relaxation and contraction (Cooke et al., 1982; Barnett & Thomas, 1989). The initial and final anisotropies are higher in contraction than in relaxation, indicating that the submicrosecond ($\phi \leq 1$ μs) disorder is smaller and/or the static ($\phi > 1$ ms) orientation is altered in contraction, probably due to

Table V: Amplitudes of Rotational Motion[a]

state	one-cone model	two-cone model	
		fast	slow
relaxation	22 ± 2°	17 ± 1.5°	12.5 ± 1°
contraction	21 ± 1°	17 ± 1°	11.5 ± 2°
attached in contraction			
70%	21 ± 2°	17 ± 2°	12 ± 2°
35%	22 ± 2°	16 ± 2°	14 ± 2°

[a] Semicone angle Θ_d (Figure 1) obtained from the anisotropy amplitudes (Table IV), using eq 3 and 4, as discussed in the text. The first column shows the results of assuming one overall motion, while the second and third columns are based on two modes of rotational motion, corresponding to the fast (r_1, ϕ_1) and slow (r_2, ϕ_i) decay components in Table IV. The first two rows correspond to a direct analysis of relaxation and contraction (Figure 3a and top part of Table IV), while the bottom two rows correspond to the different decays assuming 70% or 35% of heads attached in contraction (Figure 6 and Table VI).

actin's restriction of myosin head rotation during force generation. Further analysis of the rotational amplitudes is more model dependent. For example, if we assume that there is no static disorder in relaxation or contraction, i.e., $\delta\Theta_s = 0$ (Figure 1), we can then calculate Θ_s from the experimental value of r_∞. The Θ_s values thus obtained for relaxation and contraction are 50.4° and 48.4°, respectively. When these Θ_s values are input into eq 3, the calculated r_0 values for relaxation (0.065) and contraction (0.076) are in excellent agreement with the observed values (Table IV). Thus, the data are consistent with a small (2°) change in the static orientation in going from relaxation to contraction. However, several other models, including decreased amplitude of submicrosecond rotation in contraction, are also consistent with the data. Experiments with higher time resolution and with other fiber orientations would provide more complete information, resulting in a less model dependent description of the rotational motions (Vogel & Jähnig, 1985).

Since the anisotropy decays in both relaxation and contraction are fit much better by two correlation times than one, it is reasonable to assume that each correlation time corresponds to an independent mode of rotational motion, modeled as a wobble in a cone (Eads et al., 1984; Ludescher et al., 1987a). As in the case of previous studies of eosin-labeled myosin (Eads et al., 1984) and myofibrils (Ludescher & Thomas, 1988), this type of analysis is justified because of the large difference between the correlation times ϕ_1 and ϕ_2. The effective r_0 and r_∞ (to be input to eqs 3 and 4) were determined for each decay component as described by Eads et al. (1984). The results of this analysis are shown in Table V. The two modes of rotational motion appear to have significant amplitudes in both relaxation and contraction. Activation decreases the amplitude of the fast motion and increases that of the slow motion.

State Heterogeneity. Up to this point, we have modeled our data with the implicit assumption that each myosin head is undergoing essentially the same motions, allowing for the possibility of more than one degree of freedom (two microsecond rotational motions plus static orientation). However, the complexity of the cross-bridge ATPase cycle suggests strongly that the steady-state population of heads is biochemically and mechanically heterogeneous; i.e., several biochemical/mechanical states may have significant populations in the steady state of isometric contraction. Therefore, some of the complexity of the anisotropy decay could be due to the presence of more than one population with different motional states. As a first step in considering motional heterogeneity, following the suggestion of previous EPR work (Cooke et al.,
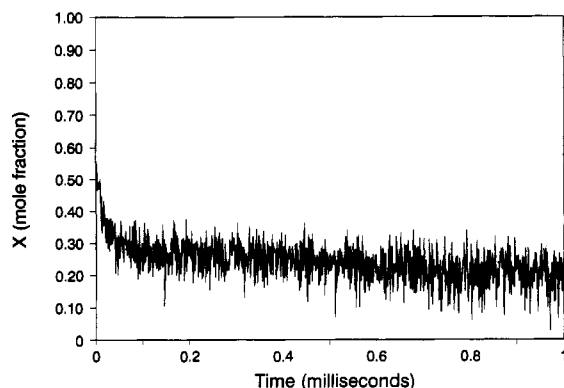
FIGURE 4: Time dependence of $x(t)$, the fraction of the anisotropy decay in rigor $[r_{rig}(t)]$ contributing to the decay in contraction, assuming that the contraction decay at each point is a linear combination of the decays in rigor and relaxation (eq 5): $x(t) = [r_{con}(t) - r_{rel}(t)]/[r_{rig}(t) - r_{rel}(t)]$. The observation that x is dependent on t implies that the motions occurring in contraction are not a simple sum of those occurring in rigor and relaxation.

1982; Fajer et al., 1988; Barnett & Thomas, 1989), we have analyzed our anisotropy decays to determine whether the decay in contraction (r_{con}) could be a linear combination of those in rigor (r_{rig}) and relaxation (r_{rel}), i.e.

$$r_{con}(t) = xr_{rig}(t) + (1 - x)r_{rel}(t),$$
$$\text{so } x = [r_{con}(t) - r_{rel}(t)]/[r_{rig}(t) - r_{rel}(t)] \quad (5)$$

where x is the mole fraction of the rigor decay that contributes to contraction. If the results obey this expression, i.e., if x is constant over the entire observed time window, a straightforward interpretation would be that a fraction (x) of cross-bridges bind in a rigid, rigorlike orientation, with the remaining cross-bridges either detached or attached with the same mobility and orientation as in relaxation. As shown in Figure 4, x is approximately 0.2 over much of the 1-ms time window, indicating that, to a first approximation, the decay in contraction is 20% rigorlike, consistent with previous EPR results (Cooke et al., 1982; Barnett & Thomas, 1989). However, the plot of x vs time is not flat, with x decaying from 0.55 to 0.25 in the first 100 μs. Since the anisotropy decay in contraction is not a linear combination of those in rigor and relaxation, the motions of the cross-bridges are different from those seen in rigor and relaxation.

One of the most important problems is to determine which motions in contracting fibers correspond to actin-attached cross-bridges, since only they can be generating force. This requires a measure of the fraction of attached cross-bridges. It has been suggested that the instantaneous stiffness, divided by that of rigor, is an accurate measure of the fraction of attached cross-bridges (Goldman & Simmons, 1977), since all myosin heads are rigidly attached to actin in rigor (Thomas & Cooke, 1980). We measured the stiffness of single labeled muscle fibers under the conditions of our phosphorescence measurements, obtaining a stiffness value in contraction of 70 $\pm$ 12% of the stiffness in rigor. The results for unlabeled fibers were not significantly different. This result is consistent with previous stiffness measurements on both unlabeled fibers (Goldman & Simmons, 1977) and spin-labeled fibers (Barnett & Thomas, 1989; Fajer et al., 1990). Using the fraction of rigor stiffness (f_{ST}) as a measure of the number of attached cross-bridges, we can obtain the anisotropy decay of the attached cross-bridges during contraction by subtracting the decay for relaxation from the decay for contraction: $r_{att}(t) = r_{con}(t) - (1 - f_{ST})r_{rel}(t)$. This plot (Figure 5, "70%") indicates that attached heads in contraction are rotationally mobile, with
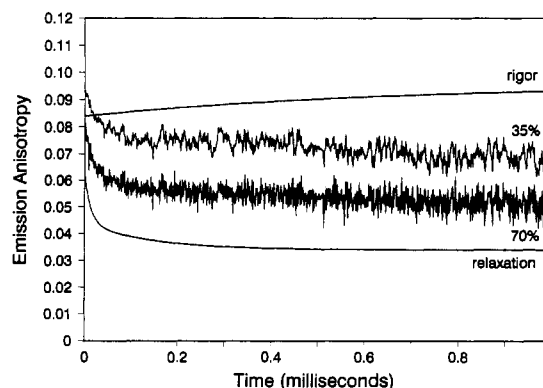

FIGURE 5: Phosphorescence anisotropy decay for attached heads during isometric contraction, assuming that the fraction of attached heads is given either by the fraction of rigor stiffness (f_{ST}) during contraction (70%) or by half this value, assuming single-headed attachment in contraction (35%). These two decays were obtained from the data in Figure 3, using the expression $r_{att}(t) = [r_{con}(t) - (1 - f_{ST})r_{rel}(t)]/f_{ST}$. The data for $f_{ST} = 0.35$ (single-headed attachment) was smoothed for display with no change in the fit parameters. Residual plots and χ^2 values showed that a two-exponential function (eq 2 with $n = 2$) provided the optimal fit in each case. The best fits to a two-exponential function are shown in Table IV. The best fits to the decays in rigor and relaxation are shown for comparison.

Table VI: Anisotropy Parameters for Attached Cross-Bridges in Contraction[a]

attached in contraction	r_1	ϕ_1	r_2	ϕ_2	r_∞	r_0	χ^2
70%	0.014	178			0.052	0.066	1.121
	0.019	25.8	0.011	878	0.047	0.077	0.977
35%	0.015	444			0.066	0.081	1.134
	0.016	20.3	0.013	598	0.066	0.093	1.105

[a] The results of fitting the difference decay (Figure 5), obtained by assuming that the fraction of attached heads is given by either the fraction of rigor stiffness (0.70) or half that value for single-headed attachment (0.35) and that the decay of detached heads in contraction is the same as in relaxation (see legend to Figure 5).

correlation times of about 25 and 900 μs (Table VI, "70%"). The amplitudes of these slower motions (Table V) are similar to those calculated from the overall decays in relaxation and contraction. If both heads of each cross-bridge are attached during contraction, contributing equally to stiffness, then this result corresponds not only to the motion of attached cross-bridges but also to that of attached heads.

Alternatively, the fraction of attached *heads* in contraction could be less than the fraction of rigor stiffness; i.e., some heads could bear more stiffness in contraction than they do in rigor. Evidence that this is possible comes from combined EPR and stiffness data from fibers in the presence of AMPPNP (Fajer et al., 1988) and pyrophosphate (Pate & Cooke, 1988), where up to half of the heads (presumably one head per cross-bridge) can be detached without a significant loss of stiffness. If only one head of each cross-bridge is attached in contraction and bears the same stiffness as a two-headed cross-bridge in rigor, then our estimate (from stiffness) for the fraction of attached heads in contracting fibers decreases to 35%. If we subtract 35% rather than 70% of the decay in relaxation, we obtain a decay of the attached heads in contraction that indicates more restricted motion (Figure 5, Table V, "35%") but still much more motion than in rigor. It is possible that the fraction of attached heads in contraction is even lower than 35%. For example, this fraction could be 21%, corresponding to the nearly constant value of x from 100 μs to 1 ms (Figure 4); but this is unlikely, since it would imply that the average attached head in contraction bears at least 60% more stiffness

than the average entire cross-bridge in rigor.

A more definitive description of attached head motions will require a more direct measure of head attachment under spectroscopic conditions. This goal seems most obtainable in solution studies of S1 and actin, where the fraction of attached heads can be measured directly by sedimentation experiments (Berger et al., 1989). Further studies correlating head rotations to the ATPase and mechanical cycles, possibly involving transient biochemical or mechanical perturbations or nucleotide analogues, will be required to clarify the motions of the attached heads and their functional role. Nevertheless, it appears that attached myosin heads in contraction undergo microsecond rotational motions that do not occur in rigor, and these motions are slower and more restricted than those occurring in relaxation.

Relationship to Other Optical Anisotropy Decays. Time-resolved studies of cross-bridge dynamics in fibers using fluorescent probes are sensitive to motions on a much shorter time scale. For example, the probe 1,5-IAEDANS attached to SH1 in fibers has a lifetime of only 20 ns (Burghardt & Thompson, 1985), so only the first 100 ns can be studied accurately. In studies of vertically oriented fibers, Burghardt and Thompson (1985) found no detectable nanosecond motion in rigor but were able to detect the initial part of a decay in relaxation with an apparent correlation time on the order of 1 μs. The amplitude of this decay, and decays corresponding to slower motions, could not be detected due to the short lifetime. The present study overcomes this difficulty by employing a phosphorescent probe with a predominant lifetime of nearly 1 ms (Table III), providing anisotropy data with high signal to noise ratio over the entire time window from 1 μs to 1 ms.

Our previous phosphorescence anisotropy results on myofibrils (Ludescher & Thomas, 1988) are consistent with the present results on fibers. For myofibrils in rigor [Figure 2b in Ludescher and Thomas (1988)], the anisotropy shows a slight rise but no decay in the microsecond time scale, as observed for fibers (Figure 3a of the present study), indicating that all heads are rigidly immobilized in rigor. The initial anisotropy level in vertically oriented fibers (present study) is only slightly less than that in randomly oriented myofibrils (Ludescher & Thomas, 1988), suggesting (from eq 3) that the angle of the emission transition moment relative to the fiber axis (Θ_s) in rigor is only slightly greater than the magic angle of 54.7° (Vogel & Jähnig, 1985). The results from relaxed myofibrils are similar to those of relaxed fibers, although in fibers the amplitudes are less and the correlation times are greater. This could indicate more restricted cross-bridge rotation in fibers than in myofibrils, but a more likely explanation is based on the effects of fiber orientation. While both azimuthal (twisting about the fiber axis) and axial (tilting relative to the fiber axis) rotations can contribute to the anisotropy decay in randomly oriented myofibrils, only the axial components of rotations can contribute to the decay in vertically oriented fibers. Two correlation times are clearly resolved in the microsecond time range in both relaxation and contraction. It is not yet possible to assign these motions unambiguously to specific structural components and rotational modes, but the shorter correlation time is probably that of the head and possibly part of S2, whereas the longer correlation times probably correspond to larger scale rotations of the cross-bridge or to a less mobile (less flexible) conformation (Ludescher et al., 1988).

The rotational motion of eosin-labeled heads, in filaments made from purified myosin, has also been measured by time-resolved absorption anisotropy (Eads et al., 1984; Ludescher et al., 1987a, 1988). Absorption measurements are essentially equivalent to the emission anisotropy experiments in the present study, but absorption detection provides a shorter dead time, providing useful data starting 50 ns after the laser pulse (Ludescher et al., 1987a; Thomas, 1986). In the time window from 50 ns to 50 μs, eosiniodoacetamide-labeled myosin heads rotate with correlation times of about 1 and 5 μs (Eads et al., 1984; Ludescher et al., 1988). These correlation times are shorter than those detected by phosphorescence in myosin filaments and relaxed myofibrils (Ludescher & Thomas, 1988) and in relaxed fibers (present study). This difference probably arises mainly from two factors: (a) the shorter time window may bias the results toward shorter correlation times; (b) the probe is different, so its transition moments may be oriented differently relative to the rotational diffusion axes.

Relationship to EPR. Many studies of cross-bridge rotation have employed spin labels attached to myosin heads [reviewed by Thomas (1987)], but the only one that addresses directly the microsecond rotational motions of myosin heads in contracting fibers is a recently published saturation-transfer EPR (ST-EPR) study employing a maleimide spin label attached to SH1 (Barnett & Thomas, 1989). Consistent with the present phosphorescence results at 4°, ST-EPR at 20° showed that the spin labels are all rigid in rigor (effective correlation time greater than 1 ms), rotationally mobile in relaxation (effective correlation time 10 μs), and almost as mobile in contraction (effective correlation time 25 μs). In steady-state ST-EPR, the effective correlation times are based on the assumption of a single isotropic rotational motion, and there is little or no information to distinguish amplitude effects from rate effects (Thomas, 1986), so a direct comparison with time-resolved phosphorescence data is not possible. This is partly remedied by conventional EPR measurements on the same spin-labeled fibers, which can resolve the orientational distribution of the probe relative to the fiber axis (Thomas & Cooke, 1980; Barnett et al., 1986; Fajer et al., 1990). A conventional EPR study on oriented muscle fibers (Cooke et al., 1982) showed that the orientational distribution is very broad in relaxation and is slightly more restricted in contraction, consistent with the increase in residual phosphorescence anisotropy (Figure 3). Both conventional (Cooke et al., 1982) and saturation-transfer (Barnett & Thomas, 1989) EPR spectra in contraction at 20° were approximated well by a linear combination of spectra in rigor (12–22%) and relaxation (78–88%). A more quantitative analysis has shown that the orientational distribution in contraction is not strictly a linear combination of those in rigor and relaxation and that the rigorlike fraction is even smaller at 4° than at 20° (Fajer et al., 1990). The present phosphorescence study confirms that the rotational dynamics in contraction are more similar to relaxation than rigor, but time resolution shows much more clearly that distinct motions are occurring in contraction (Figure 4 and Table V). The high stiffness of contracting fibers suggests that many of these dynamic myosin heads are attached to actin, and this hypothesis is supported by the observation of microsecond rotations of spin-labeled S1 still bound to actin after photolysis of caged ATP (Berger et al., 1989), and spin-labeled fibers in relaxation at low ionic strength (Fajer et al., 1985).

Conclusion. In the time window from 1 μs to 1 ms, eosin-maleimide rigidly bound to the myosin head is rigidly immobilized in rigor, rotationally mobile ($\phi = 10$ and 150 μs) but restricted in amplitude in relaxation, and less mobile (ϕ

= 20 and 300 μs) with a larger restriction of amplitude in contraction. The anisotropy decay in contraction is not a linear combination of those in rigor and relaxation, indicating that distinct motions occur in contraction. This result and the high stiffness in contraction suggest that much of the rotational motion seen in contraction involves cross-bridges that are attached to actin. These results are consistent with the hypothesis that in contraction there is a large population of attached cross-bridges that are dynamically disordered (Huxley & Kress, 1985). The results are also consistent with the proposal that a rapid rotation of cross-bridges among several attachment angles could help explain force transients observed in quick-release experiments (Huxley & Simmons, 1971). To obtain more complete information about the dynamic disorder and static orientation of the labeled myosin heads, future measurements must be done on fibers at different tilt angles relative to the excitation polarization. Higher time resolution will also be required to obtain a more complete description of the rotational dynamics of the cross-bridge during force generation. Experiments with phosphorescent probes bound to other sites will be needed to determine whether (a) the motions of the labeled domain are characteristic of the whole head, (b) labeling this site modifies cross-bridge motions, or (c) motions are induced in actin as well as myosin.

REFERENCES

Austin, R. H., Chan, S. S., & Jovin, T. M. (1979) *Proc. Natl. Acad. Sci. U.S.A. 76*, 5650–5654.

Barnett, V. A., & Thomas, D. D. (1989) *Biophys. J. 56*, 517–523.

Barnett, V. A., Fajer, P. G., Polnaszek, C. F., & Thomas, D. D. (1986) *Biophys. J. 49*, 144–147.

Berger, C. L., Svensson, E. C., & Thomas, D. D. (1989) *Proc. Natl. Acad. Sci. U.S.A. 86*, 8753–8757.

Burghardt, T. P. (1985) *Biophys. J. 48*, 623–631.

Burghardt, T. P., & Ajtai, K. (1985) *Proc. Natl. Acad. Sci. U.S.A. 82*, 8478–8482.

Burghardt, T. P., & Thompson, N. L. (1985) *Biochemistry 24*, 3731–3735.

Bürkli, A., & Cherry, R. J. (1981) *Biochemistry 20*, 138–143.

Cherry, R. J., Cogoli, A., Oppliger, M., Schneider, G., & Semonza, G. (1976) *Biochemistry 15*, 3653–3656.

Cooke, R. (1986) *CRC Crit. Rev. Biochem. 21*, 53–118.

Cooke, R., Crowder, M. S., & Thomas, D. D. (1982) *Nature 300*, 776–778.

Eads, T. M., Thomas, D. D., & Austin, R. H. (1984) *J. Mol. Biol. 179*, 55–81.

Fajer, P., Fajer, E., Svensson, E., Brunsvold, N., Wendt, C., & Thomas, D. D. (1985) *Biophys. J. 47*, 380a.

Fajer, P., Fajer, E., Brunsvold, N., & Thomas, D. D. (1988) *Biophys. J. 53*, 513–524.

Fajer, P., Fajer, E., & Thomas, D. D. (1990) *Proc. Natl. Acad. Sci. U.S.A. 87*, 5538–5542.

Garland, P. B., & Moore, C. H. (1979) *Biochem. J. 183*, 561–567.

Goldman, Y. E., & Simmons, R. M. (1977) *J. Physiol. 269*, 55P–57P.

Gornall, A. G., Bardawill, C. J., & David, M. M. (1949) *J. Biol. Chem. 177*, 751–766.

Highsmith, S., Mendelson, R. A., & Morales, M. (1976) *Proc. Natl. Acad. Sci. U.S.A. 73*, 133–137.

Huxley, A. F., & Simmons, R. (1971) *Nature 233*, 533–538.

Huxley, H. E., & Kress, M. (1985) *J. Muscle Res. Cell Motil. 6*, 153–161.

Ishiwata, S. I., Kinosita, K., Jr., Yoshimura, H., & Ikegami, A. (1987) *J. Biol. Chem. 262*, 8314–8317.

Jovin, T. M., Bartholdi, M., Vaz, W. L. C., & Austin, R. H. (1981) *Ann. N.Y. Acad. Sci. 366*, 176–185.

Kinosita, K., Ishiwata, S., Yoshimura, H., Asai, H., & Ikegami, A. (1984) *Biochemistry 23*, 5963–5975.

Ludescher, R. D. (1984) Ph.D. Dissertation, Chapter 3, University of Oregon, Eugene, OR.

Ludescher, R. D., & Thomas, D. D. (1988) *Biochemistry 27*, 3343–3351.

Ludescher, R. D., Eads, T. M., & Thomas, D. D. (1987a) in *Optical Studies of Muscle Cross-bridges* (Baskin, R. J., & Yeh, Y., Eds.) pp 33–66, CRC Press, Boca Raton, FL.

Ludescher, R. D., Peting, L., Hudson, S., & Hudson, B. S. (1987b) *Biophys. Chem. 28*, 59–75.

Ludescher, R. D., Eads, T. M., & Thomas, D. D. (1988) *J. Mol. Biol. 200*, 89–99.

Mendelson, R. A., & Cheung, P. (1976) *Science 194*, 190–192.

Mendelson, R. A., Morales, M., & Botts, J. (1973) *Biochemistry 12*, 2250–2255.

Mendelson, R. A., Putnam, S., & Morales, M. (1975) *J. Supramol. Struct. 3*, 162–168.

Pate, E., & Cooke, R. C. (1988) *Biophys. J. 53*, 561–573.

Svensson, E. C., & Thomas, D. D. (1986) *Biophys. J. 50*, 999–1002.

Thomas, D. D. (1987) *Annu. Rev. Physiol. 49*, 691–709.

Thomas, D. D., & Cooke, R. (1980) *Biophys. J. 32*, 891–906.

Thomas, D. D. (1986) in *Techniques for the Analysis of Membrane Proteins* (Ragan, R. I., & Cherry, R. J. Eds.) pp 377–431, Chapman and Hall, London.

Thomas, D. D., Seidel, J. C., Hyde, J. S., & Gergely, J. (1975) *Proc. Natl. Acad. Sci. U.S.A. 72*, 1729–1733.

Thomas, D. D., Seidel, J. C., & Gergely, J. (1979) *J. Mol. Biol. 132*, 257–273.

Thomas, D. D., Ishiwata, S., Seidel, J. C., & Gergely, J. (1980) *Biophys. J. 32*, 873–890.

Titus, M. A., Ashiba, G., & Szent-Györgyi, A. G. (1989) *J. Muscle Res. Cell Motil. 10*, 25–33.

Vogel, H., & Jähnig, F. (1985) *Proc. Natl. Acad. Sci. U.S.A. 82*, 2029–2033.

Yanagida, T., Kuranaga, I., & Inoue, A. (1982) *J. Biochem. 92*, 407–412.

Zannoni, C., Arconi, A., & Cavatorta, P. (1983) *Chem. Phys. Lipids 32*, 179–250.